ISSI science team report on developmeny A Reference Quality Model For Ocean Surface Emissivity And Backscatter From The Microwave To The Infrared.

S.J. English[1], C. Prigent[2], B. Johnson[3], S. Yueh[4], E. Dinnat[5], J. Boutin[2], S. Newman[6], M. Anguelova[7], T. Meissner[8], M. Kazumori[9], F. Weng[10], A. Supply[2], L. Kilic[2], M. Bettenhausen[7], A. Stoffelen[11], C. Accadia[12].

[1] ECMWF; [2] CNRS, France; [3] UCAR/ JCSDA, USA; [4] NASA/JPL, USA; [5] NASA/GSFC, USA; [6] MET OFFICE, UK; [7] NRL, USA; [8] RSS, USA [9]; JMA, Japan; [10] CMA, China; [11] KNMI, Netherlands; [12] EUMETSAT.

Abstract

On the 20th to 22nd of November 2019 an international science team of the International Space Science Institute (ISSI) met to discuss the challenge of developing a community reference quality ocean emission and reflection model for use across a broad spectral range (microwave and infrared, and possibly also visible) as well as supporting passive and active remote sensing. The need for this has been identified in various reports and international workshops. Notably the European Commission Horizon2020 project, GAIA-CLIM, identified in Deliverable D6.11 that the lack of a reference quality ocean emission and backscatter model was a major gap in our ability to provide absolute calibration of the satellite based observing system. The gap was also identified by the ECMWF-JCSDA radiance assimilation workshop in December 2015 and the 21st meeting of the International TOVS Working Group in December 2017.

An international science team was proposed to ISSI and accepted, to develop a new model capability with these goals and characteristics : That it have or be,

- Maintained and supported;
- Have traceable uncertainty estimation at each step;
- Be documented code freely available to research community;
- Have new science for IR to MW with BRDF capability;
- Support passive and active applications.

The ISSI team noted the state of the art in the science for each component of such a model and the applicability over such a wide range of wavelengths. The considered what work it would take to deliver the ambitious goal and formed a plan of action to deliver this over the next few years. This includes a number of stages, delivering less ambitious new capability initially, but keeping in mind always the goal of covering all aspects. A key component of this was to deliver a model whose uncertainty was fully characterised, traceable to SI standards where possible, but in all cases documented as fully as is realistic. This will support use of observations in a very broad range of applications, where the absolution calibration of the model (as well as the observations themselves) is of critical importance.

This report highlights the key findings of the first meeting of the science team and outlines the plan how to create this new community software. It describes the work required to combine state of the art elements already available with new aspects in order to create a complete model. This model would serve both the scientific research community by enabling better reference calibration for observations in climate applications and also to train fast models for operational

applications such as numerical weather prediction (NWP). In section 2 the reader is reminded of the theoretical basis for different components of the model. In section 3 models used in real-life practical applications are described, many of which have to make compromises and assumptions. In section 4 the evaluation of the uncertainty of these model is discussed, and the plan to attempt to deliver the goals of the science team are described in section 5.

The reports and findings of the ISSI team are available at http://www.issibern.ch/teams/oceansurfemiss/.

2. Theoretical basis of models

2.1 Geometric optics (Prigent)

A summary of the development, range of applicability and current issues was presented to the meeting and is summarized below.

The sea surface interaction with the radiation can be simulated with geometric optics models. The ocean surface is described as a collection of flat surfaces with a bi-directional slope distribution. Each facet reflects specularly the downwelling brightness temperature, following the Fresnel laws. These models can be applied from the visible to the microwaves, in both passive and active modes. The sea surface response is mainly a function of wind speed and direction and surface temperature. It requires statistics about the surface slope distribution, the dielectric properties of the sea water, the foam characteristics (both coverage and emissivity), and information about the downwelling radiation.

In passive microwave, the geometric optics models have a long history, starting in the 60's with theoretical developments by Stogryn (1967), evaluated with measurements by Nordberg et al. (1969) or Hollinger (1971), in the 1 to 19 GHz range. These comparisons already showed the significant role of the foam on the emissivity (Nordberg et al., 1969; Webster and Wilheit, 1976), as well as the frequency dependent sensitivity to the wave spectrum (Hollinger, 1971). The Cox and Munk (1954) slope variances, derived from visible observations of the Sun glint over the ocean was widely adopted. Addition of the effect of small scale roughness superimposed on the large scale slopes was suggested by Wentz (1975), to improve the model at low frequencies. The geometric optics approach was used at large scale for the analysis of the first passive microwave observations for oceaniability c purposes, from 6 to 37 GHz, with the Scanning Multi-channel Microwave Radiometer (SMMR) (e. g., Wilheit, 1979). Since then, several versions of the geometrics optics models have been developed and used (e. g., Prigent et Abba, 1990 ; Phalippou, 1996 ; Guillou et al., 1996), showing good agreement with observations, especially at frequencies above 37 GHz. Below 37 GHz, the use of only a fraction of the Cox and Munk (1954) slope variance is suggested. Slope shadowing, multiple reflection at the surface as well as wind direction can, to some extent, be considered in these geometric optics approaches. More recently, a parameterization of a geometric optics model has been proposed, to estimate the sea surface emissivity up to 700 GHz, for the new instrument (the Ice Cloud Imager) planed for the European MetOp-SG satellite. This parameterization (the Tool to Estimate the Sea Surface Emissivity in the Microwave and Millimeter waves TESSEM[2]) is now included in the RTTOV package (Prigent et al., 2017).

For the simulations of active microwave observations, the geometric optics models have shown serious limitations for observing incidence angles above 15°, where the Bragg scattering dominates the signal (e.g., Mouche et al., 2005; Nunziata et al., 2009). As a consequence, these models are not suitable for the analysis of scatterometer or SAR data.

In the infrared, geometric optics methods have been adopted with success. The emissivity shows a rather slowly decrease with little effect of the wind speed, below 30° incidence angle (e. g., Masuda et al., 1988; Wu and Smith, 1997).

Regardless of the frequency range and model types, critical input parameters are required: the geometric optics model does not escape the rule, despite its simplicity. A large range of sea wave spectra are available in the literature. The sea surface large scale roughness is governed by the gravity waves. The variance of the slopes estimated by Cox and Munk (1954) has been widely used. Spectra such as the Durden and Vesecky one (1985) have also been adopted, often with a multiplicative coefficient on the slope variance that depends upon the authors. For the sea water dielectric properties, in the infrared as well as in the microwaves, different parameterizations have been suggested, based on lab measurements. Recent measurements have been performed at 1.4 GHz (Zhou et al., 2017), but not in the other frequency ranges, despite remaining large uncertainties. The foam characteristics, both its coverage and emissivity, have a strong impact on passive microwave observations (much less in active microwaves and in the infrared), especially at high wind speeds. A large range of parameterizations are available, and efforts should be conducted to propose a consistent physically-based approach (e.g., Anguelova et al., 2013). Group discussions about these three aspects (wave spectrum, sea dielectric properties, and foam) will be reported later. The processing of the downwelling radiation over the ocean surface is also to be accounted with great care in the modeling of the sea surface response. The downwelling radiation in the specular direction is not the only contribution, especially at 1.4 GHz, where extra-terrestrial contributions from different directions have to be estimated in addition to the cosmic background (Galaxy, Sun, Faraday rotation, that are all varying in time and space).

2.2 Two scale models (Yueh)

The progress on the physical modeling of microwave emission from sea surfaces was reviewed. The two-scale scattering models were established in 1960s-1980s for ocean radar and radiometer remote sensing, e.g., Semyonov (1966), Wu and Fung (1972), Wentz (1975) and Durden and Vesecky (1985) with applications to the assessment of ocean surface wind of microwave backscatter and brightness temperatures. In 1990s, the model was extended to account for the directional dependence of vertically and horizontally polarized brightness temperatures (Irisov et al., 1992). The model was further extended to polarimetric emissions, characterized by four Stokes parameters (Yueh , 1997), which has become the basis of ocean surface emissivity module for operational weather forecasts analysis. In the two-scale scattering model, the Bragg scattering by small-scale waves contributes to bistatic incoherent scattering and modifies the coherent reflection coefficients of large-scale waves. A critical part of the two-scale models is the sea surface spectrum. The major difference between various two–scale scattering models is the representation of sea surface spectrum, such as (Pierson and Stacy, 1973; Fung and Lee, 1982; Donelan and Pierson, 1987; Apel, 1994; Elfouhaily et al., 1997; Kudryavtsev et al., 1999; Wackerman et al., 2002; Kudryavtsev et al., 2003a; Kudryavtsev et al., 2003b). The improvement of two-scale models over time is largely due to the advances in the characterization of sea surface spectrum. In addition to wind speed and direction, additional sea surface parameters, such as wave age, have been introduced in the since 1990s.

The one proposed by Elfouhaily et al. (1997) has been popular, used by many studies, likely due to its ease of implementation and representation of first-order physics. The limitation of this spectrum, as well as many others, is the applicable range of microwave frequencies. They allow reasonable agreement between two-scale model simulations and radar data at C and Ku-band, but yield poor performance at lower or higher frequencies. For example, the application of Elfouhaily's spectrum to L-band (~1 GHz) backscatter computation will lead to a negative wind speed sensitivity for a certain range of wind speed, inconsistent with observations (Yueh et al., 2013; Yueh et al. 2014). Tuning to the spectrum coefficients becomes necessary to improve agreement with remote sensing radar and radiometer observations from L-band to Ka-band and higher frequencies.

In addition, many experimental observations have shown the influence of waves on microwave backscatter and emissions (Nghiem et al., 1995, Quilfen et al., 2004; Gabarro et al., 2004; Yueh et al., 2015). The parameterization of wave effects in the sea surface spectrum remains lacking. The shape of sea surface spectrum and dependence on various sea state parameters still require further research.

A well-recognized weakness of the two-scale model is the empirical selection of the two-scale cutoff wavenumber to divide the surface roughness spectrum into two parts for short and long waves. The recent advancement in Numerical Maxwell equation 3-Dimensional (NMM3D) surface scattering has helped address this issue. The two-scale cutoff wavenumber has been nominally chosen to be in the range of one third to one fifth of the electromagnetic wavenumber by various investigators. Using a higher cutoff will allow a larger long wave slope, and hence more tilting surface effects, but will leave a larger gap for microwave backscatter computation at low incidence angles. The NMM3D simulations performed by Qiao et al. (2018) show that the choice of one third of the electromagnetic wavenumber for the cutoff will allow agreement between model and L-band radar data, in support of the empirical selection by many investigators for microwave ocean scattering and emission. The advances in rigorous numerical techniques for solving scattering from realistic 3-dimensional rough surfaces have confirmed the fundamental basis of two-scale models and will help independent validation of the two-scale models over a broader range frequencies, and hence allow us to address the contribution of other surface features or roughness drivers, such as breaking waves, boundary-layer stability and hydrodynamic modulation of short wave by long waves.

Two-scale models do not account for the contribution of foam (or white cap), which is known to be a bright radio emission source for 19 to 37 GHz microwave frequencies. L-band radiometer measurements performed by the (Camps et al., 2004) during the WISE campaigns indicated that the presence of sea foam will introduce a net increase of about 10K for Tv and 5K for Th at about 40-50 degree incidence angles and 1.41 GHz frequency for 100 percent foam-covered sea surfaces. Sea foam influences sea surface brightness temperatures over a very wide frequency spectrum, and is indispensable for sea surface emissivity modeling. However, the impact of sea foam varies with electromagnetic frequencies with differing penetration into sea foam, a mixture of water and air bubbles. Hwang et al. (2019) examined several airborne and satellite radiometer datasets and proposed a sea-foam emission model that can be combined with the two-scale model to produce a semi-empirical microwave sea surface emissivity model, accounting for the impact of roughness and foam. Their result is promising and can be considered as the first step for inclusion into the community sea surface emissivity model. Further assessment using independent datasets will be essential, in particular for applications to extreme high winds (Yueh et al., 2016).

2.3 Foam models (Anguelova)

A summary of the development, range of applicability and current issues was described to the meeting and is summarized below.

Both bubble rafts floating on the surface (whitecaps) and bubble plumes below the surface constitute sea foam. While bubble plumes are important for gas exchange and turbulent mixing, the whitecaps on the surface are of interest for remote sensing. The emissivity of these surface foam patches was the subject of this presentation.

Foam layers on the surface comprise closely packed bubbles with wide range of sizes. Bubble size distribution thus characterizes sea foam in terms of microscopic variables (e.g., bubble radius and bubble wall thickness). Void fraction (the amount of air contained in air-seawater mixture) and foam layer thickness describe sea foam in terms of macroscopic variables. These two sets of variables are connected because having the bubble size distribution we can always obtain the foam void fraction.

The most important feature of the sea foam layers is the formation of a void fraction profile because of the stratification of bubbles by size: large, thin-walled bubble cluster at the top of the foam layer due to their buoyancy; small, thick-walled bubbles settle at the bottom. This specific mechanical structure of the sea foam brings in vertical variations of the air-seawater content in foam layers depth. This, in turn, yields the radiative properties of foam, which support the strong, black-body-like emissivity of foam-covered seawater.

The high emissivity of foam-covered areas comes from two main components, namely (i) the presence of a medium with high attenuation (thus emission) of electromagnetic (EM) radiation; (ii) effective propagation of the EM radiation to the attenuating medium. In the foam-seawater system, the highly absorptive seawater is the former while the vertically stratified sea foam is the latter. The high emissivity of foam-covered areas cannot be guaranteed if one of these two components were missing. For high absorption (and emission) by seawater cannot be realized if the large dielectric contrast between the air and seawater is not smoothed by the foam impedance matching, and vice versa: Effective transfer of EM radiation across the foam layer boundaries with the air and seawater is not enough if a lossy medium is not in place to absorb it.

Absorption and scattering attenuate the EM radiation interacting with the foam-seawater system. The contributions of absorption and scattering to the attenuation (radiative losses) depend on the size parameter x, which relates the sizes of the scattering bubbles to the wavelength of the propagating EM radiation. The scattering magnitude determines the approach to modeling the attenuation in foam. Scattering is weak to negligible for $x < 1$; it increases for $x \geq 1$. Therefore, we can ignore the scattering for low frequencies (from L band up to 40 GHz), but need to account explicitly for losses due to scattering for high, millimeter wave frequencies (40 to 200 GHz).

Knowing the foam mechanical structure and the radiative processes governing the foam losses, one can prescribe requirements for developing a radiative transfer model (RTM) for foam emissivity. Review of known foam emissivity models shows that none of them follows all prescribed requirements. In fact, this is not necessary when the specific application of a foam emissivity model allows sensible assumptions and simplifications. NRL developed a foam emissivity RTM heeding this premise.

Foam emissivity RTM for low frequencies represents the foam properties with a void fraction profile; currently, this profile has fixed upper and lower limits of 99% and 1%, respectively. This structural profile is then combined with the effective medium theory to obtain the attenuation in foam; result show that the foam absorption losses dominate. These then are used in the incoherent approach, applicable for weakly scattering media, to compute the foam emissivity. Finally, these computations are generalized for a range of foam layer thicknesses using log-normal probability distribution. The resulting foam emissivity is weakly dependent on radiation frequency and polarization. However, comparisons of modeled emissivity to experimental data at 1.4, 10.8 and 35 GHz show that close correspondence can be achieved when the upper limit of the void fraction varies with frequency.

Foam emissivity RTM for millimeter wave frequencies is similar with one essential change, namely rigorous scattering theory must be used to calculate the attenuation in foam. NRL uses Generalized Multi-particle Mie (GMM) theory to account for the interaction and interference between the electric fields of the closely packed bubbles comprising the foam layers. The GMM theory is well validated experimentally. Initial results for the attenuation of foam streaks (with characteristic length scales from 2 mm to 10 m) show that foam is still emissive medium with absorption losses dominating the scattering. However, the scattering losses monotonically increase for frequencies above 40 GHz contributing more than 25% to the total attenuation (extinction).

Future work on modeling the foam emissivity includes: further improvement of the foam RTM, especially on modeling the frequency and polarization dependences; choice of whitecap fraction parameterization, which scales the relative contribution of sea foam to the total ocean emissivity; and approaches to assess the uncertainties of foam emissivity and whitecap fraction. These topics were discussed.

3. Models used in operational and research applications

3.1 The LOCEAN model (Boutin)

A summary of the LOCEAN model was presented to the meeting and is summarized below.

The 'LOCEAN' sea surface emissivity model has been developed with the aim of retrieving Sea Surface Salinity (SSS) from SMOS (Soil Moisture and Ocean Salinity) L-band radiometric measurements. It has two components, the dielectric model and the model for wind induced effects.

a. Dielectric constant model

Dinnat et al. (2019) have evidenced systematic Sea Surface Temperature (SST) related differences between satellite SSS and in situ SSS when satellite (SMOS or Aquarius) Tb are adjusted to the Klein and Swift (1977) dielectric constant model. We found at least two origins for these systematic differences:

- A conditional sampling effect due to the noise on the reference SST

- Issue with the dielectric constant model : Pseudo dielectric constant derived from SMOS measurements (Waldteufel et al. 2004) allows to revise Klein and Swift parametrization by either adjusting the static dielectric constant or the fresh water relaxation time parameters: analysis of higher frequency measurements would allow to distinguish between the two parametrizations.

b. Wind and wave aspects

The model of Yin et al. (2016) involves two components:

- The roughness emissivity is modelled with a 2-scale emissivity model following Yueh (1997). The multiplicative coefficient of the wave spectrum of Durden and Vesecky (1985) has been adjusted to better fit SMOS brightness temperatures (Tb) between 3 and 7m/s where it is assumed that foam impact is small: it is equal to 1.25 instead of 2 in Yueh (1997).
- A foam model has been added to describe SMOS Tb between 7 and 22m/s. The angular dependency of SMOS Tbs (ranging between nadir and 55° incidence) has been used to constrain parameters of the Anguelova and Gaiser (2013) foam emissivity model: Void fraction at the air-foam interface, SMOS-Adjusted, is 0.97; Effective foam thickness is ~1.8cm. In addition, the wind speed dependence of SMOS Tb have been used to adjust the foam fraction model dependence to wind speed. Several functions have been derived depending slightly on the chosen ancillary wind speed and sea spectrum model. All functions show a significantly reduced foam fraction compared to model derived from optical measurements. In addition to the wind speed dependency, the SMOS Tb angular dependency puts strong constraints on these adjustments. Nevertheless, all these adjustments are not fully independent and it would be interesting to analyze their consistency with higher frequency observations.

3.2 The RSS model (Meissner)

A summary of the RSS model was presented to the meeting and is summarized below. As with the LOCEAN model, he RSS ocean emissivity model consists of two components, dieletric model and wind and wave aspects.

a. *Dielectric constant model*

The flat surface emission, which is given by the model for the dielectric constant of sea-water (Meissner and Wentz, 2004, 2012). The Meissner – Wentz dielectric model for pure and sea-water is a double Debye relaxation model. It covers the sea surface salinity range between 0 and 40 psu and SST range between -2°C and 32°C. The Debye parameters were fitted based on laboratory measurements at L-band and W-band. The fit was carefully edited to account for observations from passive microwave satellites (SSM/I and WindSat). More recently AMSR, GMI and the Aquarius and SMAP salinity missions have been used for validation.

b. *Wind and wave aspects*

The wind induced emissivity model: The main model covers the frequency range 6 – 90 GHz (Meissner and Wentz 2012). There is a special version for L-band (Meissner et al. 2014, 2018). The RSS wind emissivity model contains and iso-tropic (wind direction independent) component and a wind-direction signal for all 4 Stokes parameters. The model parameters depend on frequency, polarization, Earth incidence angle, wind speed and SST. They were fitted based on observations from SSM/I, WindSat and the recent Aquarius and SMAP L-band missions. In addition, it includes a term (Omega term) that accounts for the atmospheric path-length correction of the reflected downwelling radiation. For L-band sensors there are a variety of additional sources that need to be included in the forward RTM calculation (e.g. reflected galaxy and sun, Faraday rotation in the Earth ionosphere).

The model has been extensively validated through:

1. Analysis of measured versus RTM calculated brightness temperatures from a variety of passive microwave sensors (see Figure 1). The best calibrated sensors are GMI and WindSat.

2. Comparison of environmental parameters that are retrieved from satellite observations using the RSS emissivity model with in-situ data. See Figure 2, which compares WindSat wind speeds with buoy measurements. Other validation examples that were performed include:

- Comparison of AMSR or WindSat SST with buoys.
- Water vapor measurements from SSM/I, WindSat, AMSR or GMI with GPS observations.
- Ocean surface salinity measurements from Aquarius and SMAP with ARGO drifters.

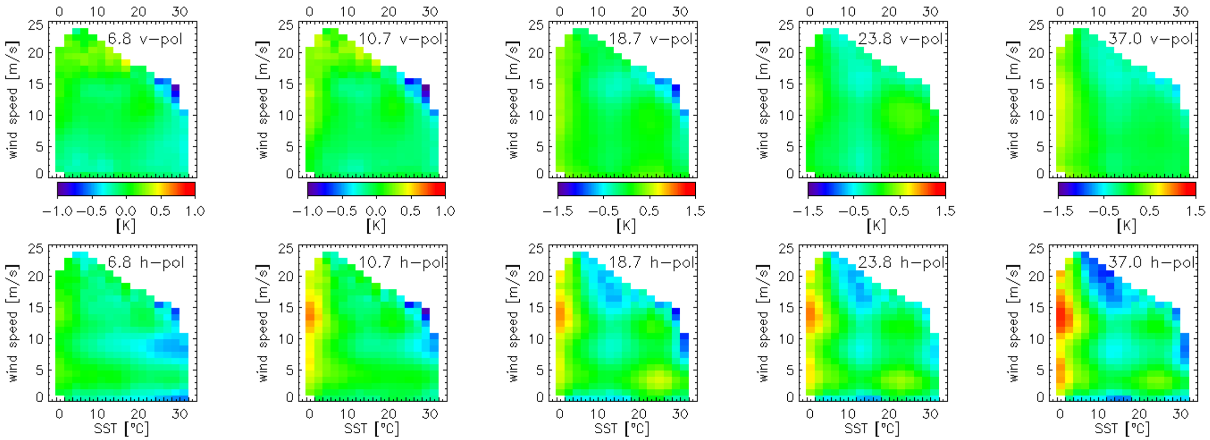

Figure 1: TB measured – calculated for the 10 WindSat channels as function of wind speed and SST.

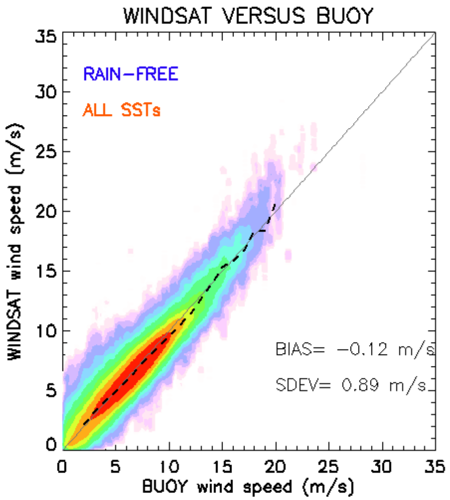

Figure 2: WindSat versus buoy wind speed.

3.3 The Fastem model and RTTOV (English, Newman)

The Fastem model was developed specifically with fast calculations in the framework of data assimilation of raw radiances in an Numerical Weather Prediction system. The requirements were therefore speed of computation, availability of gradient code (K, tangent-linear and adjoint), ability to reproduce as accurately as possible the outputs of a slower offline model, but with a clear trade-off between speed and accuracy meaning the latter may sometimes be compromised. The verison version (English and Hewison, 1998) was written with the AMSU-A instrument in mind, optimised for accurate computations for a cross-track sounder with frequencies between 20 and 90 GHz, with best accuracy around 50 GHz. Following uptake of Fastem version 1 at many NWP centres interest grew to improve its accuracy for conical scanning imagers, notably SSM/I and SSMIS, which led to Fastem version 2 (Deblonde and English, 2001). Fastem version 3 was a minor adjustment to add an azimuthal variation. As Fastem was not well designed to work below 20 GHz or above 100 GHz, work was undertaken (Liu, Weng and English, 2011) to extend its range of applicability, especially as it was already being widely used for MHS and other observations at 183 GHz. This, theoretically at least, extended the range of applicability to 1-200 GHz. This was initially implemented in Fastem version 4, but some undesirable behaviours were seen, notably for the Foam modelling, leading to improvements in these aspects in Fastem version 6. Finally, Kazumori and English revisited the azimuthal variation and found it to not be correctly implemented from Fastem version 4 onwards, and a new formulation was added. The successive versions of Fastem are listed in Table 1.

Fastem Version	Permittivity (1 change, poss 2nd)	Roughness (4 changes)	Foam (0 changes, 1 temporary, 1 additional capability tested)
1	Ellison et al 1998	GO / specular Regression fit	Monahan and O'Muircheartaigh (1986)
2	Ellison et al 1998	GO + specular with "omega" term Regression fit	Monahan and O'Muircheartaigh (1986)
3	Ellison et al 1998	GO + omega + WindRad azimuthal term Regression fit	Monahan and O'Muircheartaigh (1986)
4	Liu et al 2011	2-scale + WindRad Regression fit	Tang (1974)
5	Liu et al 2011	2-scale + WindRad Regression fit	Monahan and O'Muircheartaigh (1986)
6	Liu et al 2011	2-scale + Kazumori (2015) azimuthal term Regression fit	Monahan and O'Muircheartaigh (1986) + wave model option

Table 1 : Changes in Fastem versions 1-6.

As an operational NWP centre, the Met Office data assimilation systems use the fast model RTTOV for radiative transfer calculations. Some recent developments in RTTOV sea surface emissivity modelling were presented. In the infrared, the IREMIS module has recently been developed (Saunders et al., 2018) to predict the sea surface emissivity as a function of zenith angle, wind speed and skin temperature. These calculations depend on a wave slope model (Masuda, 2006) adopting wave slope statistics from Ebuchi and Kizu (2002). It was noted during discussions that there is no accepted standard description for wind-induced wave slope probabilities, and other formulations such as that of Cox and Munk (1954) are often used in similar models. The presence of foam is neglected in IREMIS. Stuart presented previous work on the temperature dependence of the ocean water complex refractive index (Newman et al., 2005) which leads to a measurable impact on the emissivity near 800 cm^{-1} and is now accounted for in IREMIS.

In the microwave, RTTOV supports the FASTEM (versions 1-6) and TESSEM^2 sea surface emissivity models. FASTEM is optimised for frequencies below 200 GHz whereas TESSEM^2 is an extension up to 700 GHz. For NWP applications the emissivity is calculated as a function of 10m wind speed, skin temperature, salinity, zenith angle and azimuth angle. FASTEM outputs do not have estimated uncertainties attached, which has implications for the validation of satellite microwave sensors in the NWP framework. Stuart showed results from the recent EU project GAIA-CLIM (Gap Analysis for Integrated Atmospheric ECV CLImate Monitoring) which aimed to establish sound methods for the characterisation of satellite-based Earth Observation (EO) data using reference non-satellite data. The difference between observed and NWP model equivalent top-of-atmosphere brightness temperature (observed-background, or "O-B") is sensitive to instrument artefacts, such as orbital-dependent calibration biases seen for the MWRI sensor on FY-3C. But assessing the rigorous statistical significance of O-B statistics is difficult for microwave imagers because a large component of the uncertainty in modelled brightness temperature stems from the surface emission. Thus, although O-B differences for well-calibrated sensors such as GMI on the GPM satellite are small (< 1 K, based on Met Office and ECMWF results) there is no direct traceability in the accuracy of the comparison. GAIA-CLIM recommended that quantifications of the effects of surface properties should be improved to reduce uncertainties in satellite data assimilation, retrieval and satellite to non-satellite data comparisons. The establishment of a reference ocean emissivity model is therefore fully aligned with the needs of Earth observation community.

3.4 GMFs for active observations (Stoffelen)

For the modelling of active microwave responses off the ocean surface at incidence angles above 20 degrees, the detailed spectrum in phase and amplitude of the small ocean scales needs to be modelled in order to estimate the interference of microwaves with the ocean topography in different azimuth directions. This depends on wave breaking processes and hydrodynamic modulation effects. To theoretically understand Doppler returns, the time evolution must be studied too. The uncertainty of physically-based models, which are informed by satellite microwave measurements remains relatively high at about 1dB (20%) (e.g., Fois, 2015). Nevertheless, these models are very useful for designing instruments at different wavelengths and predicting their sensitivity and performance.

This is in sharp contrast with the stable wind scatterometer instruments, that have been shown to stay within 0.1 dB (2%) over a decade. An empirical method, called cone metrics (Belmonte et al., 2017), that monitors the stability of the ASCAT measurement PDF over the ocean, measures relative linear gain differences of about 0.02 dB (0.4%) from one year to the next, where ASCAT-A over 2013 is currently taken as absolute reference for geophysical applications. QuikScat and NSCAT are currently used as de facto reference for Ku-band scatterometers.

Ground-based transponders are inaccurate for quality monitoring, but provide absolute ball-park calibration for ASCAT. Moreover, the rain forest has a daily cycle of about 15% in microwave backscatter; it may still be used for stability monitoring at given LTAN for sun-synchronous satellites. Other land targets are affected by moisture events (dew, rain), including deserts, and ice/snow targets may be stable for months, years or decades, but will be affected by melting or rain at some point in time (climate change).

Given the excellent relative calibration between instruments and the increasing collocation opportunities, excellent and consistent empirical Geophysical Model Functions (GMF) have been developed at used wavelengths, polarizations and angles. In addition, reasonable control (QC) on ancillary parameters, such as SST, atmospheric stability, ocean waves and rain have been performed, using well-known and controlled in situ and NWP references, except for extremely high winds.

The stable and accurate signal, high-quality empirical GMFs, retrieval algorithms and refined QC are implemented in generic C- and Ku-band wind processors and quality monitoring services. Wind vector component accuracies are estimated by triple collocation and typically 0.5 m/s on the measurement scale, typically 25 km.

Relative to this accuracy and on this spatial scale, NWP models have rather large systematic (Belmonte and Stoffelen, 2019) and random errors (Stoffelen et al., 2017), typically 1 m/s or more. This in itself prevents direct assimilation of backscatter data in NWP models, since relatively large random background errors would need to be propagated through the non-linear forward and inverse operators, where higher-order effects should be accounted for, which is rather cumbersome and inaccurate. In addition, background biases should be removed before data assimilation.

For wind data assimilation, Trindade et al., (2019) demonstrate a method to correct local scatterometer o-b biases that are stable over a few days, which reduced overall global o-b variances by 20% against independent scatterometer winds. These NWP model errors are due to mesoscale air-sea interaction, e.g., due to ocean eddies and atmospheric PBL modelling in both convective and stable conditions, and have substantial large-scale components too. The correction method allows in principle 1) substantial corrections to the data assimilation process by removing local biases and 2) improved ocean forcing by correcting ocean forcing errors.

In summary, scatterometer backscatter calibration and wind data processing are well under control and steps can now be taken for improved NWP wind data assimilation and hence forecast impact, by improved exploitation of the scatterometer winds. The empirical GMFs are the basis for physically-based modelling of the behaviour of gravity-capillary waves on the ocean surface, which is useful for the development of new instrument specification.

3.5 CRTM ocean emissivity model application (Johnson)

The Joint Center for Satellite Data Assimilation (JCSDA) Community Radiative Transfer Model (CRTM) is a fast, 1-D radiative transfer model used in numerical weather prediction, calibration / validation, and satellite simulation, spanning multiple federal agencies and universities. The key benefit of the CRTM is that it is a satellite simulator, in that it provides a highly accurate representation of satellite radiances by making appropriate use of the sensor-specific instrument response functions convolved with a line-by-line radiative transfer model (LBLRTM). CRTM covers the spectral ranges consistent with all present operational and most research satellites, from visible to microwave. The capability to simulate ultraviolet radiances are being added over the next two years and will become available in CRTM version 3.0. Another unique aspect of the CRTM is that it also provides the tangent-linear, adjoint, and Jacobian outputs needed for satellite data assimilation applications. The ability to compute a Jacobian for various geophysical input parameters significantly expands the capabilities beyond traditional forward RT models There are two primary requirements for an operational radiative transfer model: speed and accuracy. To accelerate computations, the CRTM heavily relies on pre-computed lookup tables for clear-sky transmittance, clouds, surface, and aerosol properties.

In particular, fast and accurate computation of the surface radiative properties pose specific and unique challenges. In CRTM version 2.3 (present operational version), the treatment of the ocean surface is divided into three categories: solar-impacted radiances, thermal infrared radiances, and microwave radiances. For solar radiance impacted channels, a "rough seas" bidirectional reflectance distribution function (BRDF) is used, which provides the specular and Fresnel reflection angles based on the Cox and Munk slope approximation. For thermal infrared, the Infrared Sea-Surface Emissivity model (IRSSE) is used, as described initially in Nalli et al., 2008. In the IRSSE, the wave-slope model is based on Ibuchi and Kizu (2002), and refractive indices from Wieliczka (1989). For microwave radiance simulations over water, we make use of a slightly modified version of the FASTEM-6 model, described previously. The zenith angle dependent foam reflectivity follows section d of Kazumori (2008), and uses the azimuthal emissivity model of Kazumori (2015). The dielectric properties are described by Liu (2010). For foam coverage, the model of Monahan and O'Muircheartaigh (1986) is used, under the assumption of neutral stability (i.e., the near-surface air temperature is equivalent to the surface skin temperature). The large scale and small scale correction components are similar to that of FASTEM.

The Community Surface Emissivity Model (CSEM). a library of existing surface emissivity models, has been integrated with the CRTM to enable the modification and testing of various selections of land and ocean models, however, this integration is not yet operational.

CRTM 3.0 will support full polarization radiative transfer capabilities. This will support polarized atmospheric scattering, and surface reflection / emission through modified BRDFs. This capability Is under development in coordination with NESDIS/STAR researchers. Significant development efforts will focus on the development of a generalized surface module to handle scalar and vector forms of the BRDF, particularly in support of the polarization effects of the physical variations of the ocean surface temperature/salinity dependent dielectric properties, wave height spectra, small scale corrections, foam coverage and emissivity, and wind-speed impacts. This will also provide support for active sensor observations of the ocean surface, such as the Normalized Radar Cross-Section (NRCS), and polarization induced by off-nadir radar beam reflections.

3.6 ARMS ocean emissivity model applications (Weng)

A fast and accurate radiative transfer model is required for assimilation of satellite data into numerical weather prediction model. In Chinese numerical weather prediction models, RTTOV is operationally used for assimilating NOAA, EUMETSAT and CMA satellite data. In the next decade, more advanced instruments will be carried onboard Chinese FengYun satellites and will provide more data for various applications. Fengyun satellites in the geo and leo orbits are becoming a vital component for consterllation of the global observing system. Many instruments are unqiue to the international users and include a geostationary hyperspectral infrared sounder at the spectral coverage of 4-15 micron and a geostationary microwave imaging sounder having a frequeny covering from 50-450 GHz. At the geostationary platform, a large solid apenture will be deployed for obtaining atmospheric temperature sounding at a resolution comparible to that from the current polar microwave sounder such as Advanced Microwave Sounding Technology Sounder (ATMS) and Microwave temperature Sounder (MWTS). To accelerate uses of current and future FengYun satellite data, CMA is now developing a new generation of Advanced Radiative transfer Modelling System (ARMS) in preparing for the new mission (Weng et al., 2020). ARMS has the capabilities similar to RTTOV and CRTM but design with more flexibilities for pluging new radiative transfer solvers, using of new scattering data bases of aerosols, clouds and precipitation, and interfacing with other fast models such as CRTM and RTTOV. Its instrument coefficients can be used by both CRTM and RTTOV.

Currently, both ARMS and CRTM use FASTEM-6 for simulations of microwave radiance over oceans. For a cross-track scanning instrument such as Suomi NPP ATMS, the biases (O-B) between observations and simulations across the scan angle can exhibit an omega shape under clear conditions for surface sensitive channels (Weng and Yang, 2016). The O-B for upper air sounding channels is nearly independent of scan angle. This pattern could result from either an emitting antenna or angular dependent ocean emissivity error. Thus, it is required that a reference ocean emissivity model be developed to separate the bias contributed from the emitting antenna from that from the in accurate surface emissivity model.

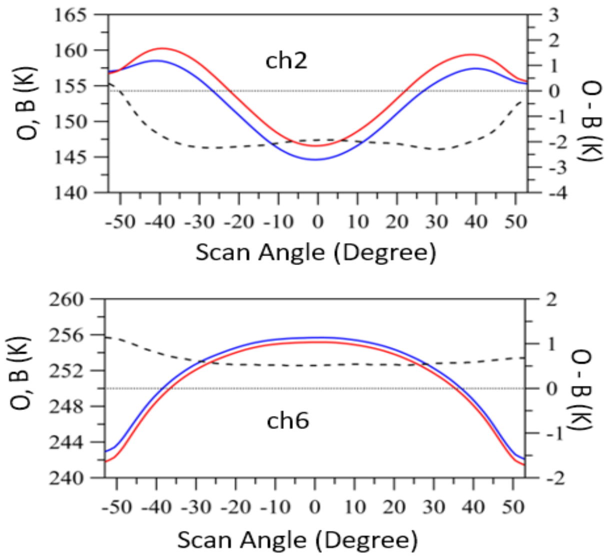

Figure Captions: ATMS channels 2 (upper panel) and channel 6 (lower pannel) mean angular dependent observation (O, solid blue color), simulation (B, solid red) and the difference (O-B, dash black) between O and B. Simulated sensor brightness temperatures (SDR) are based on NCEP global forecast model 6 hour forecast fields and the mean values are averaged from all the data over the ocean surfaces during the period of December 20-26, 2011. Only those data sets are used for CLW less than 0.03 kg/m^2, total precipable water less than 10 kg/m^2 and surface wind speed of less than 7 m/s. The brightness temperatures are labled in left Y-axis and the O-B in right Y-axis, and the scan angle is labled at the x-axis

The radiance emitted from the antenna subsystem can also complicate the O-B distribution and result in the maginutde difference between satellite ascending and descending nodes. For the earlier launched instrument such as SSMIS on board DMSP F16 and F17 satellites, the reflector emission can be complicated by the reflector face temperature cycle dominated by solar panel Shadowing for most of year, some earth and spacecraft shadowing, reflector heating due to solar reflections off of spacecraft body. SSMIS O-B patterns also showed frequency dependent reflector emissivity, have 1.5–2K O-B jump at 50-60 GHz, 5-7K Jump at 183 GHz when the satellite is out of the earth eclipse. The actual bias of SSMIS imaging channels was not accurately quanfitied due to lack of a high fidelity of surface emissivity model. For some microwave imagers (e.g. FY-3 MWRI and AMSR-2), the reflector emission is significant and a large O-B difference and its node-dependence can be readily identified from RTTOV simulations with FASTEM.

4. Evaluation of models compared to requirements

4.1 Evaluation of LOCEAN, RSS and Fastem models (Kilic)

Three different ocean Radiative Transfer Models (RTMs) from 1.4 to 89 GHz to satellite observations from SMAP and AMSR2 were evalusted by Kilic et al., 2019. This comparison exercise required the development of a dataset of satellite observations from SMAP and AMSR2, collocated with surface and atmospheric parameters. Consistent ECMWF ERA-Interim and Mercator reanalysis data are chosen. The database samples the global oceans over a year.

The selected ocean RTMs are (1) the LOCEAN RTM developed for the SMOS mission (Dinnat et al., 2003 and Yin et al., 2016) (2) the FAST microwave Emissivity Model (FASTEM) version 5 parameterized from a full physical model (Liu et al., 2011), (2) the Remote Sensing System (RSS) empirical model, fitted with SSM/I and WindSat observations between 6 and 9 GHz (Meissner and Wentz 2004, 2012) and with Aquarius at 1.4 GHz (Meissner et al., 2014, 2018).

The simulations were carefully compared to the observed Brightness Temperatures (TBs). Firstly, global systematic errors between simulations and observations were computed. The biases tend to increase with frequency, and are generally higher at horizontal than at vertical polarizations. This is partly due to the increasing effect of the atmospheric contribution with frequency (essentially undetected clouds), especially at horizontal polarization. Part of it, can also stem from AMSR2 calibration issues. Secondly, the analysis focused on the accuracy of the RTMs as a function of the key ocean variables, Sea Surface Temperature (SST), Sea Surface Salinity (SSS), and Ocean Wind Speed (OWS) (once the global biases are subtracted).

Major discrepancies with the observations were found at frequencies above 1.4GHz, for OWS higher than 7m/s, with the LOCEAN and the FASTEM models, with differences strongly increasing with increasing OWS. Possible model improvements were discussed. The analysis tended to show that a frequency dependence needs to be added to the foam cover model or / and on the foam emissivity model. The study also stressed that these two components have to be considered consistently and jointly, all over the frequency range. Efforts should be devoted to the modeling of the foam contribution, taking into account the OWS, but also the frequency dependence, and possibly the wave dissipative energy.
Cold SSTs were also identified as a source of disagreement between the simulations and the observations, regardless of the model. This is a critical issue, especially at vertical polarization at 6 GHz which is the key channel for the SST analysis from satellite. Large uncertainties still exist in the modeling of the dielectric constants of sea water, particularly at low SSTs. New laboratory measurements of the dielectric properties of ocean water have recently been undertaken at 1.4 GHz: their extension to higher frequencies should be encouraged, insisting on the uncertainty estimation.

4.2 Evaluation and improvements of the microwave ocean surface emissivity model FASTEM (Kazumori)

An empirical relative wind direction (RWD) model function to represent azimuthal variations of oceanic microwave radiances of vertical and horizontal polarizations was developed. The RWD model function was based on radiance measurements from the Advanced Microwave Scanning Radiometer and Special Sensor Microwave Imager/Sounder (SSMIS). Ocean surface wind vector data from SeaWinds on board the Advanced Earth Observing Satellite-II and European Centre for Medium-range Weather Forecasts (ECMWF) Integrated Forecasting System were utilized for the RWD model function development. The RWD model function was introduced to a microwave ocean emissivity model, FAST microwave Emissivity Model (FASTEM). FASTEM is a radiative transfer model for satellite radiance assimilation. Performances of the RWD model function were much more realistic than previous azimuthal model functions in FASTEM for low wind speed and high-frequency channels. Assimilation experiments using the RWD model function were performed in the ECMWF system. The experiment demonstrated reductions of first-guess departure biases arising from modelling of the azimuthal variations in areas of high wind-speed and low variability of wind direction. For example, bias reductions in ascending and descending SSMIS 19 GHz vertically polarized radiance in the Somali jet over the Arabian Sea were approximately 0.6 and 0.7 K. The bias reductions were found for all assimilated microwave imager channels in a wide wind-speed range. Moreover, analysis increments of specific humidity in the lower troposphere were reduced (e.g. 0.2 g kg^{-1} reduction at 1000 hPa in the Somali jet). Improvements of relative humidity and temperature in short-range forecasts in the lower troposphere were found. The experiment results clearly showed the importance of modelling the azimuthal variation of emissivity for assimilation of microwave imager observations. The new RWD model function, combined with the other components of FASTEM, is available as FASTEM-6.

4.3 Consistency of various microwave SST products with SMOS measurements in the Arctic Ocean (Supply)

Sea surface salinity (SSS) retrieval in the Arctic Ocean is particularly challenging due the low signal to noise ratio of L-band brightness temperatures with respect to SSS in cold waters and to the presence of ice (Yueh et al. 2001; Meissner et al. 2016; Tang et al. 2018). Sea surface temperature (SST) retrieval and validation is also difficult in this area because of the presence of clouds, variability of the sunlit time and the lack of in-situ data (Minnett et al. 2019). Nevertheless, SST is used as a prior information in the SSS retrieval and is critical in order to retrieve SSS with a minimum level of uncertainty. We investigate in this presentation the importance of difference between prior SST, used for Soil Moisture and Ocean Salinity (SMOS) SSS retrieval, and in-situ SST measurements and we present a methodology allowing to correct SST-induced bias using another SST product as a reference.

The presented study uses a various set of in-situ salinity and temperature measurements recorded in the Arctic Ocean between 2011 and 2017. Argo and CTD profiles, and underway thermosalinographs (TSG) measurements are combined in order to represent as much as possible the different regimes encountered in the Arctic Ocean. Concerning satellite data, SMOS L2 (ESA v662) is used for SSS. For SST, on one hand we consider the European Centre for Medium-Range Weather Forecasts from the Integrated Forecast System (ECMWF) SST which are used as a prior in SMOS SSS processor. They are derived from OSTIA foundation SST the day prior to SMOS measurement and brought down to one-meter depth and to the time of SMOS measurement using a trend estimated with ECMWF coupled model. We compare these SST with Remote Sensing Systems (REMSS) foundation SST (http://www.remss.com/measurements/sea-surface-temperature/oisst-description/).

Comparison of REMSS and ECMWF SST with in-situ measurements demonstrated a more negative difference between ECMWF SST and in-situ temperature compared to REMSS SST. We observe very similar tendency when comparing OSTIA and REMSS foundation SST. This difference is more pronounced in the river plumes areas where strong gradients of SST are recorded. In case the difference between ECMWF SST and in-situ temperature is important, SMOS SSS also strongly differ from in-situ salinity.
A correction is applied to SMOS SSS in the Arctic Ocean to estimate the influence of SST errors. Using REMSS SST as a new reference, the SSS difference induced by the difference between REMSS SST and ECMWF SST is estimated given the partial derivative of SMOS Tb relative to SSS and SST.
A new SMOS SSS product is developed for Arctic Ocean using this SST-related correction. Mean difference between SMOS SSS and in-situ SSS is reduced by 50% (0.8pss) over the arctic Ocean and STD differences are reduced in river plumes areas (from 1.8 to 1.1 pss in the Laptev Sea).
This study highlights the importance of using a SST prior consistent with L-Band radiometric measurement for retrieving SSS in the Arctic Ocean.

4.4 Evaluation of ocean emissivity models for polarimetric microwave radiometers (Bettenhausen)

Polarimetric microwave radiometers with channels in the 10-37 GHz frequency range provide the capability to retrieve ocean surface vector winds (OSVW) which was first demonstrated from space using the WindSat instrument (Gaiser, 2004; Bettenhausen, 2006). The same instruments can also provide observations useful for tropical cyclone imagery and retrieval of other geophysical parameters including sea ice age and concentration, snow water equivalent, sea surface temperature and soil moisture. In addition to WindSat which continues to operate after launching in 2003, two additional polarimetric microwave radiometer missions are planned to provide OSVW measurements beginning in the early 2020'ss: Compact Ocean Wind Vector Radiometer (COWVR) (Brown, 2017) and the Weather System Follow-on - Microwave (WSF-M) (Ball, 2017).

An accurate model of the emissivity of the wind roughened sea surface including the effects of sea foam is needed to support OSVW retrieval from polarimetric radiometer brightness temperatures (Tbs). Accurate modeling of the wind speed and wind direction dependence of the emissivity of the third and fourth Stokes Tbs is particularly important because the Tb signal is less than or on the order of 1 K. The third and fourth Stokes Tb sensitivities to atmospheric and ionospheric effects and sea surface temperature are much smaller than the sensitivity to OSVW.

The United States Naval Research Laboratory (NRL) developed an emissivity model (Bettenhausen, 2006; Bettenhausen, 2017) specific to WindSat frequencies and earth incidence angles (EIA) to support WindSat OSVW retrievals. Remote Sensing Systems (RSS) has developed a more general emissivity model (Meissner, 2012) for frequencies between 6 and 90 GHz and EIA less then 65°. The NRL and RSS models for the third and fourth Stokes emissivity are empirically derived primarily using WindSat Tbs. The two models were developed independently using different sets of WindSat data and different OSVW “ground truth” data. Both models use a two term odd-sinusoidal Fourier series in the wind direction relative to the instrument azimuthal look direction to approximate the Tbs where the harmonic terms vary with wind speed.

A comparison of the two models for the WindSat EIAs and frequencies of 10.7, 18.7 and 37 GHz show good agreement for wind speeds less than 20 m/s. Comparisons are made between the models in terms of the product of the emissivity and SST. The largest difference is that the RSS model assumes a zero first harmonic for the fourth Stokes emissivity whereas the term is up to about 0.2 K at wind speeds above 15 m/s in the NRL model. The models agree to less than about 0.1 K for all three frequencies for the third Stokes harmonics and the and fourth Stokes second harmonic. These comparisons provide confidence that these emissivity model for the third and fourth Stokes provide a good benchmark for development of a reference emissivity model.

4.5 Comparison of models for sea water dielectric constant and wind (surface roughness and foam) at low microwave frequencies (Dinnat)

We assess the performance of a semi-theoretical radiative transfer model for ocean emissivity/reflectivity for reproducing brightness temperature (TB) observations from several microwave sensors between the frequencies 1.4 GHz and 36 GHz. The electromagnetic component of the model is the two-scale model which parts ocean roughness scales into small and large scales according to their size compared to the sensor's electromagnetic wavelength. Several dielectric constant models for sea water and wind (i.e. surface roughness and foam) are tested. Data from sensors operating at L-band (1.4 GHz) and C- (7 GHz) , X- (10 GHz) and K/Ka-bands (24 GHz, 36 GHz) are used to assess the model parameterizations. The objective is to optimize a model based on physical principles to use for simulations of the ocean surface emissivity and reflectivity at microwave frequencies.

We assess the model performances

- at L-band, by comparing sea surface salinity (SSS) satellite retrievals to *in situ* measurements,
- at L-, C-, X- and K/Ka-bands by comparing simulated surface TB and top-of-atmosphere TB to satellite observations.

We use the satellite TB from the SMAP L1B V4 and the AMSR2 L1A products; and the SSS and TB from the Aquarius L2 products. The *in situ* salinity observation are from the Argo network.

Dielectric constant models assessed are from (Ellison et al., 1998; Ellison et al 2003; Klein & Swift, 1977; Meissner & Wentz, 2012; A. Stogryn, 1997; A. P. Stogryn et al., 1995; Zhou et al., 2017). We find that:

- TB from the various models differ by at most 1.5 K (L-band) to 2 K (other frequencies);
- There are differences in TB dependence to SST, which are most significant at low frequencies due to the reduced signal from SST. The differences in simulated TB at all frequencies vary by ~1K across the all temperature range (–2°C to 30°C). But the total change in TB across SST at L-band is only ~2 K, while it is much larger at C- (25K) and X- (18K) band.
- The model from GWU (Zhou et al., 2017) based on recent laboratory measurements exhibits the smallest error estimates with the Aquarius SSS retrievals (+/- 0.15 psu). However, the model relies on data at L-band only; its use at higher frequencies is unvalidated. The MW model (Meissner & Wentz, 2012) is close in accuracy to the GWU model on SSS retrievals (+/- 0.25 psu) and has been developed and validated over a large range of frequencies (up to 90 GHz).

For the wind model, we compare the performances of the widely used sea spectrum model by (Durden & Vesecky, 1985) [DV85] to the model by (Yin et al., 2016) [Yin2016] developed recently using SMOS TB data at multiple incidence angles and 2 polarizations. The Yin2016 model uses the DV85 model multiplied by a factor 1.25 for the sea spectrum, the foam emissivity model of (Anguelova & Gaiser, 2013) and foam fraction model adjusted to fit SMOS data at the higher winds. We find the Yin2016 model to provide good performances with the other L-band sensors (SMAP, Aquarius), especially at V-pol. H-pol show small differences with Aquarius GMF above 8 m/s but the overall dependence to wind speed is reasonable. The DV85 alone (i.e. no foam) Is too linear compared to the observations. Adding a historical foam model (emissivity and foam fraction) to the DV85 spectrum results in too large changes of TB with wind speed. Yin2016 reduced the foam fraction at L-band arguing that the penetration depth at low frequency resulted in less effective foam being sensed.

At higher frequencies (C-, X-, K and Ka bands), the Yin2016 wind model shows decreased performances; its dependence on wind speed is too small. Using the historical foam fraction model by (Monahan & O'Muircheartaigh, 1986) significantly improves the performances at all the frequencies above L-band. Overall we find that the DV85 model multiplied by 1.25 coupled with the foam emissivity model by (Anguelova & Gaiser, 2013) and a foam fraction that is frequency dependent provides good performances at multiple frequencies. More tests are needed to ensure optimum selection of the model parameters and consistency of the model when used for surface reflection for applications to active instrument.

A good agreement between a physics based radiative transfer model and radiometric observations was found. Adjustment to a limited number of model parameters was needed. The foam model is found critical in ensuring good performances across frequencies. The approach adopted here was to adjust the foam coverage model at low frequencies in order to decrease the amount of foam being sensed by the radiometer. Other approaches are possible, such as adjusting the foam effective thickness or the void fraction at the air/foam interface. These approaches will need to be evaluated to identify the method that produces the best results at all polarizations, incidence angles and frequencies. Assessing the model performances with active sensor will also be important to validate the underlying physical assumptions.

4.6 Emission model requirements for next generation satellite instruments (Accadia)

The previous sections have presented a detailed discussion on the current capabilities in terms of surface emissivity modeling and supporting observations in the microwave range. In this respect, The EUMETSAT Polar System - Second Generation (EPS-SG) will continue and enhance the capabilities already available from the Metop satellites. For EPS-SG a number of missions have been identified, which include the Micro-Wave Sounding (MWS) mission, the Micro-Wave Imaging mission (MWI), the Ice Cloud Imaging (ICI) mission, and the SCAtterometry mission (SCA). More details on these missions can be found in the respective Science Plans, available at: https://www.eumetsat.int/website/home/Data/ScienceActivities/ScienceStudies/SciencePlansforfuturemissions/index.html. EPS-SG missions offer new measurement possibilities. MWI and ICI microwave and sub-mm wave conical imaging missions are on the same platform, together with the SCA. The SCA instrument is a C-band scatterometer.This allows for synergy, since MWI measurements can be collocated with SCA measurements in order to characterize sea surface roughness and even beam filling conditions. Moreover, SCA offers V- and H-polarized measurements on the mid-beam, allowing for wind measurements up to hurricane force (>30 m/s). Thus, these measurements will offer new opportunities to further improve ocean emissivity models, but they will also pose new challenges. For example, assimilation of data (either at L1 or L2) from SCA and MWI over the same area will require physical consistency between the backscatter model at C band and the emissivity model. Moreover, ICI will observe at high frequencies, e.g. the 243 GHz channel, where it is likely to observe the surface in some atmospheric conditions, as documented in a scientific study in preparation for the new observations on board EPS-SG. In the frame of the same study, a parameterization of the sea surface emissivity has been proposed from 10 to 700 GHz: TESSEM2 (Tool to Estimate Sea Surface Emissivity from Microwave to sub-Millimetre waves) (Prigent et al., 2016). It is based on the community model FASTEM (English and Hewison, 1998; Liu et al., 2011) at frequencies up to 200 GHz where FASTEM has been operationally calibrated and validated. It follows a physical emissivity model at higher frequencies (Prigent and Abba, 1990). A preliminary evaluation of TESSEM2 has been conducted by comparison with airborne International Sub-Millimetre Airborne Radiometer (ISMAR) observations from 118 to 325 GHz, under low wind speed (3 to 5 m/s) off the coast of Scotland. TESSEM2 is a fast parameterization that can easily be implemented in a community radiative transfer model: it is available to the community and is implemented in RTTOV. This is however, a first step, and it is expected to be updated once ICI will be operational.

Another relevant future mission in this context is the Copernicus Imaging Microwave Radiometer (CIMR) mission, currently in development at phase B2. CIMR has been identified by the European Space Agency (ESA) as one of the High Priority Expansion Missions in support of the Arctic Policy of the European Commission (EC). CIMR will be implemented as a high spatial resolution polarimetric conical imager providing information on the full Stokes vector, with channels from 1.4 GHz up to 36.5 GHz. Thus an additional clear requirement for future emissivity models is to be capable to accurately represent the full polarimetric contribution of the ocean surface.

It is worth mentioning that several applications would benefit from a solid and shared reference ocean emissivity model: of course data assimilation, but also Cal/Val activities and radiance observation monitoring in-flight, Level 2 retrievals (e.g. use in 1D-Var LWP retrieval), or simulation studies of new satellite sensors. It shall be anyway compatible for an implementation within RTTOV or another operational RTM. Finally, quite some effort shall be dedicated also to validate the reference surface emissivity model.

5 Discussion

5.1 Permittivity models (session chair: Thomas Meissner)

Several sea-water permittivity (dielectric) are currently being used in microwave RTM calculations and for retrieving environmental parameters:

1. Klein – Swift model (Klein and Swift 1977): The Klein-Swift model was one of the first sea-water permittivity model for microwave frequencies and it is still widely used. It is a single Debye relaxation model. The Debye parameters were fitted based on laboratory measurements at low frequencies. It can be used for frequencies below Ku-band, but the single Debye fit becomes increasingly inaccurate at higher frequencies. As no cold SST (below 5°C) were used in the parameter fit, The Klein-Swift model becomes also inaccurate at very low SST.
2. Meissner – Wentz model (Meissner and Wentz 2004, 2012): The Meissner – Wentz dielectric model for pure and sea-water is a double Debye relaxation model. It covers the sea surface salinity range between 0 and 40 psu and SST range between -2°C and 32°C. The Debye parameters were fitted based on laboratory measurements at L-band and W-band. The fit was carefully edited to account for observations from passive microwave satellites (SSM/I and WindSat). More recently the model has also been tested and used for retrievals with AMSR, GMI and the Aquarius and SMAP salinity missions.
3. The Ellison model (Ellison et al. 1998): The Ellison model it is also a double Debye relaxation model and is based on laboratory measurements over a wide frequency range. No satellite measurements were used in its derivation. An edited version of this model is currently used in the FASTEM (Liu et al. 2011).

One major item that came up in the discussion was that it is necessary to assess the uncertainty of the permittivity models in order to be able to decide how useful the models are for radiative transfer application. Several error sources enter the derivation of the various permittivity model.
1. Random noise in the laboratory measurement: This is in general a very small component.
2. Absolute biases: They are difficult to distinguish from satellite calibration offsets and are basically taken out when calibrating the satellite to the RTM.
3. Most important are errors in the permittivity model that depend on SST and SSS. Those errors will result in cross-talk biases in environmental retrievals of SST, SSST, wind speed and water vapor.
Thomas Meissner took a up the task to assess the SST and SSS dependent uncertainties in the Meissner – Wentz dielectric model. This will be based on comparing the real and imaginary of the dielectric model as well as the flat surface emission with the results of the laboratory measurement t W-band (Guillou et al. 1998), which are regarded as very reliable as well as the recent L-band laboratory measurements by Lang et al. 2016.

5.2 Roughhness models (session chair: Simon Yueh)

There were a range of discussions on roughness scattering models for ocean radiances. Several key issues and comments associated with roughness models and implementation for fast models (e.g. Fastem) were raised. They are:

1. To date no attempt has been made to ensure physical consistency between the ocean surface roughness model used in Numerical Weather Prediction (NWP) and Climate Models and that used in radiative transfer models. The team considers effort towards improved physical consistency to be necessary.
2. The two-scale models are the basis for quantifying the roughness impact on emissivity in operational models. These two-scale models are being used routinely over a wide frequency band from 1 to 200 GHz. The accuracy and performance of models over this wide frequency band needs to be further assessed, in particular cutoff wavelength number.
3. What is the interaction of wind with small scale waves for various sea states? Wind stress is nominally understood as the principal driver of surface roughness. Several surface roughness models are available and it is unclear which is the best choice, or to what extent all are limited. There is evidence some models perform better in specific regions, suggesting that they are tuned to the conditions in that region and should not be used globally. There is therefore work needed to validate the roughness models both regionally and globally to determine the reference spectrum model. Furthermore, use of real time wave swell analysis from a numerical wave model as run at many operational centres needs to be evaluated, in order to allow correctly for the swell component of the wave spectra.
4. Physically-based models are needed to describe/understand behaviour at different wavelengths and polarizations. In the past empirical tuning to satellite or field campaign data has proven necessary to provide sufficient accuracy, both for active and passive instruments, for aspects such as:
   a. Wavelength dependency
   b. Wind azimuth and speed dependency
   c. Polarization/incidence dependency
5. The current empirical tuning approach for developing geophysical model functions (GMF), relating microwave backscatter and brightness temperatures to ocean wind speed and direction, is primarily based on the matchup of satellite data with NWP winds. Careful interpretation of the empirical model function is required since the major NWPs have been assimilating passive and active microwave data. Because the satellite wind products are effectively a

representation of wind stress, the effects of sea states, in addition to wind, have been partially accounted for in the empirical GMF. The winds as one of the inputs to the physical-based models may differ from the characteristics of NWP winds. To compare the empirical GMF with the physical-based models, we have to take the characteristics of NWP winds into consideration.

6. The characterisation and reduction of model uncertainty at high wind speed is the most critical issue for JMA, including both small scale and large-scale corrections.

5.3 Foam (session chair: Maggie Anguelova)

A number of presentations, given during the 1st science team meeting for developing a reference quality radiative transfer model (refRTM hereafter) for the ocean emissivity, overviewed the models currently in use in the remote sensing community. This overview showed a consensus in the community that a physical model for the foam emissivity should involve foam properties. The major topics related to the foam emissivity that emerged from the presentations for further discussion were: (1) Choice and further improvement of a RTM for foam emissivity $e_{f.}$; (2) Choice and further improvement of a parameterization of foam fraction (whitecap coverage) *W*; and (3) Assessing the uncertainties of $e_{f.}$ and *W*. The following is a summary of the group discussion on these three topics. For each topic, we give first the established status, then suggestions for future developments (in the year leading to the 2nd science team meeting in November 2020), and finally the agreed upon responsibilities for specific contributions by the team members.

5.3.1 Modeling foam emissivity

The overview showed that the NRL model for foam emissivity (Anguelova and Gaiser, 2013, RSE) is widely used in the community. Specific modifications and adjustments made the model applicable for different frequencies, from L band (Yin et al., 2016, RSE) up to 40 GHz (Anguelova and Bettenhausen, 2019, JGR). The model is considered also useful for high, millimeter wave frequencies (from 40 up to 200 GHz), however the work on obtaining foam attenuation due to both absorption and scattering at these frequencies is still a work in progress.

The major discussion on the future development of the model was on how best to account for the frequency and polarization variations of the foam emissivity, which are too weak in the current model implementation. Independent studies suggested that the frequency dependence of the model can be improved by varying the void fraction profile (especially its upper limit) for different frequencies. Comparisons of the current and modified foam emissivity values to available experimental data can help to better account for both frequency and polarization variations.

Anguelova took the responsibility to provide code for the foam model. Kilic has coded the model in FORTRAN90. This code will be starting point to generalize the code for a range of frequencies and, if necessary, to add (or expand) code descriptions and clarifications. Anguelova will work on modifying the foam model to include frequency dependence in the foam void fraction. Anguelova will communicate with Dinnat to coordinate and verify the quality of these modifications using data at L band. Anguelova will also continue work on foam attenuation and emissivity at millimeter wave frequencies within the framework of a currently funded project at NRL.

5.3.2 Foam fraction parameterization

The overview showed that different groups have used different parametrizations of whitecap fraction based on in situ observations of *W*. While all parameterizations are based on power law in the form $W = aU^b$, the coefficients *a* and *b* differ significantly. The aerosol community uses high wind speed

exponent of *b* = 3.41 (for the sea spray production), while the remote sensing community (including FASTEM) uses *b* = 2.55 from a formulation of *W* in terms of wind speed and atmospheric stability (the latter usually assumed neutral). It was clarified in the discussion that while cubic dependence of *W* on *U* is physically justified, numerous aerosol studies have shown that it overestimates *W* predictions at high latitudes and underestimates *W* at lower latitudes. Lower wind speed exponent is expected if the influence of additional factors, not only wind speed, affect *W.* This is further corroborated by the fact that predictions of *W* with *b* = 3.41 do not compare well with *W* values retrieved from WindSat observations, which presumably account for all factors affecting *W*. Values *W* obtained with *b* =2.55 follow the trends of satellite-based *W* data and parameterizations better. Moreover, the empirical *W* expressions, developed specifically for use at L band (Yin et al., 2016, RSE), show wind speed trends similar to those obtained with *b* =2.55. The consensus in the group was to use the *W*(*U*) parametrization from FASTEM (with *b* =2.55) and/or *W*(*U*) expressions based on satellite retrievals of *W*.
The group also discussed the need to use *W* parameterizations that include more variables, e.g., wind, atmospheric stability, SST, and wave field characteristics. Such multivariable *W* parameterizations can be obtained from satellite retrievals of *W* macthed with a range of variables characterizing various meteorological and oceanographic conditions. However, it was pointed out that satellite retrievals of *W* show strong frequency and polarization variations. While the observed frequency variation is a surrogate for whitecaps with different thicknesses, it was agreed upon that one oceanographic value for *W* should be reported.
Anguelova continues to work on satellite retrievals of *W* and a database of *W* data and additional forcing variables necessary to develop multivariable *W* parameterization. The work on modifying the frequency dependence of the foam emissivity (see point 1 above) is anticipated to diminish the frequency and polarization variations of the *W* retrievals. This should contribute to improved report of *W* values for oceanographic studies.

5.3.3 Uncertainties

This point is the most difficult to assess mostly because of lack of direct measurements of both foam emissivity and whitecap fraction. The foam emissivity uncertainty could be evaluated as the remaining differences between modeled and measured brightness temperature values when the uncertainties for seawater permittivity and sea surface roughness are assessed. Anguelova can use available in situ *W* data to evaluate *W* error. Further, comparisons of in situ and satellite *W* data can help to assess the uncertainty of *W* retrievals. The problem in this activity is time because Anguelova can make these assessments during future projects (with pending proposal funding).

6 Planning for community model development

The group agreed some specific actions to take the activity forward:

- All scientific papers to be shared amongst the group, as some are more difficult to obtain. These can be linked to from the ISSI web page.
- Ben Johnson to put up a GitHub from NOAA for the code developments. Space for some data (no more than 1THz).
- Jacqueline Boutin has plans to change the dielectric model for SMOS processing, and to do tests on the SST. This model will be made available and then evaluated.
- Maggie Anguelova has plans to change for the L band foam emissivity, with a new version of the model. She will make the code available for evaluation.

- Thomas Meissner will make additional tests on the dielectric model with Zhou measurements for low frequencies and with Liebe model for the high frequencies.
- The group reached a consensus to work with Emmanuel Dinnat's 2 scale model as a core system. The Fortran code base requires some cleaning / commenting to facilitate sharing and joint development. During the development this will only be made available to a small core team.
- The model will be compared to the model from Fuzhong Weng, who will also approach Ming Chen and Mark Liu to see if they wish to contribute to this effort.
- The two scale model will also be used to calculate IR emissivities and compared to Stu Newman's results, to see how realistic this is. In this intercomparison Stephen English will approach Nic Nalli to see if he also wishes to contribute to this validation exercise.
- A goal of the activity is not only to create a model, but also one with uncertainty estimated. Therefore in the code design we need to propagate uncertainty information from estimates of uncertainty in the model parameters.
- The group agreed that as this model aspires to be reference quality, it should not be tuned to a specific instrument, even one (e.g. GMI) that is considered to be of a higher reference quality.
- The model should also predict the wind direction component for the full Stokes vector. Windsat data and the existing RSS code can be used for validation. Mike Bettenhausen will investigate making the best quality reprocessed data available, but if not the real time data product is available e.g. archived at ECMWF.
- The group's activities are on a best endeavours basis. The NWPSAF could be approached for resources (some limited resources have been made available from the Visiting Scientist budget of the NWPSAF). All group members will investigate possible sources of funding to allow more extensive activities.
- It was noted that if the code is submitted to the IEEE system it gets a DOI number. They provide tests and keep the code. However to update a new version must be submitted (and accepted) and another DOI allocated. So this is something to do only with mature code versions, and then with major updates in the future.
- The group discussed the issue of licencing of the code? Apache-2 open source license is a possibility. All group members to consider further to enable a clear decision on this when the code reaches the point for wider dissemination.

- The next physical meeting will again be held mid-November, in 2020.
- A videocall between the team members will be organized in spring 2020 to assess progress.

References

Apel, J., (1994): An improved model of the ocean surface wave vector spectrum and its effects on radar backscatter, J. Geophys. Res., Vol. 99, No. C8, pp. 16,269-16,291, August 15.

Anguelova,M., & Gaiser, P., (2013). Microwave emissivity of sea foam layers with vertically inhomogeneous dielectric properties. Remote Sens. Environ., 139, 81–96. http://dx.doi.org/10.1016/j.rse.2013.07.017

Balana, A., Delbos, G., Lamkaouchi, K., Eymard, L., Guillou, C., & Prigent, C., (1998). New permittivity measurements of seawater. *Radio Science*, *33*(3), 639. https://doi.org/10.1029/97RS02223

Ball, (2017): Ball Aerospace Wins Major U.S. Air Force Contract for Next-Gen Weather Satellite, [Press Release]. Retrieved from https://www.ball.com/aerospace/newsroom/detail?newsid=123879.

Bell, B., English, S.J., Candy, B., Atkinson, N., Hilton, F., Baker, N., Swadley, S.D., Campbell, W.F., Bormann, N., Kelly, G., and Kazumori, M., (2008): The assimilation of SSMIS radiances in numerical weather prediction models*. IEEE Trans. Geosci. Remote Sens.,* 4, 884–900.

Bettenhausen, M.H., and Coauthors (2006): A Nonlinear Optimization Algorithm for WindSat Wind Vector Retrievals. *IEEE Trans. Geo. Rem. Sens.*, **44**, 597-610, DOI: 10.1109/TGRS.2005.862504.

Bettenhausen, M.H., and M.D. Anguelova (2017): An updated geophysical model for WindSat observations, *2017 IEEE International Geoscience and Remote Sensing Symposium (IGARSS), Fort Worth, TX*, 1224-1226, DOI: 10.1109/IGARSS.2017.8127179.

Brown, S., and Coauthors (2017): The COWVR Mission: Demonstrating the capability of a new generation of small satellite weather sensors, *2017 IEEE Aerospace Conference, Big Sky, MT*, pp. 1-7, DOI: 10.1109/AERO.2017.7943884.

Camps, A., J. Font, M. Vall-lossera, C. Gabarro, I. Corbella, N. Duffo, F. torres, S. Blanch, A. Aquasca, R. Villarino, L. Enrique, J. Miranda, J. Arenas, A. Julia, J. etcheto, V. Caselles, A. Well, J. Boutin, S. Contardo, R. Niclos, R. rivas, S. C. Reising, P. Wursteisen, M. Berger, and M. Martin-Neira, (2004): The WISE 2000 and 2001 Field Experiments in support of the SMOS Mission: Sea Surface L-band Brightness Temperature Observations and their applications to Sea Surface Salinity Retrieval, IEEE Trans. Geosci. Remote Sens.

Cox, C. and Munk, W.H., (1954): Measurements of the roughness of the sea surface from photographs of the sun's glitter. J. Opt. Soc. Am., 44, 838–850.

Cox. C., and Munk, W.H., (1956): Slopes of the sea surface deduced from photographs of sun glitter, Bull. Suipps Inst. Oceanogr., 6, 40l-499.

Deblonde, G., English, S.J., (2000): Evaluation of the FASTEM-2 fast microwave oceanic surface emissivity model. InProc. 11th Int. ATOVS Study Conf 2000 Sep 26, 67-78.

Dinnat, E.P., Le Vine, D.M., Boutin, J., Meissner, T., Lagerloef, G., (2019): Remote Sensing of Sea Surface Salinity: Comparison of Satellite and In Situ Observations and Impact of Retrieval Parameters. Remote Sens., 11, 750.

Dinnat E.P., Boutin, J., Caudal, G., and Etcheto, J., (2003): Issues concerning the sea emissivity modeling at L band for retrieving surface salinity. Radio Science, 38(4), ISSN 00486604

Donelan, M.A., and W. J. Pierson, (1987): Radar scattering and equilibrium ranges in wind-generated waves with applications to scatterometry," J. Geophys. Res., Vol. 92, No. c5, 4971-5029, May 15.

Durden, S. L., and Vesecky, J. F., (1985). A Physical Radar Cross-Section Model for a Wind-Driven Sea with Swell. *IEEE Journal of Oceanic Engineering*, *10*(4), 445–451. https://doi.org/10.1109/JOE.1985.1145133

Ebuchi, N. & Kizu, S., (2002): Probability distribution of surface wave slope derived using sun glitter images from geostationary meteorological satellite and surface vector winds from scatterometers,, Journal of Oceanography (2002) 58: 477. https://doi.org/10.1023/A:1021213331788

Elfouhaily, T., B. Chapron, K. Katsaros, and D. Vandemark, (1997): A unified directional spectrum for long and short wind-driven waves, J. Geophys. Res., Vol. 102, No. C7, 15,781-15796, July 15.

Ellison, W. J., Balana, A., Delbos, G., Lamkaouchi, K., Eymard, L., Guillou, C. and Prigent, C., (1998): New permittivity measurements of seawater, Radio Sci., 33(3), 639– 648.

Ellison, W. J., English, S. J., Lamkaouchi, K., Balana, A., Obligis, E., Deblonde, G., Hewison, T. J., Bauer, P., Kelly, G., and Eymard, L., (2003), A comparison of ocean emissivity models using the Advanced Microwave Sounding Unit, the Special Sensor Microwave Imager, the TRMM Microwave Imager, and airborne radiometer observations, J. Geophys. Res., 108, 4663, doi:10.1029/2002JD003213, D21.

English, S.J, and Hewison, T. J., (1998): Fast generic millimeter-wave emissivity model, Proc. SPIE 3503, Microwave Remote Sensing of the Atmosphere and Environment, https://doi.org/10.1117/12.319490.

Fung, A. K. and K. K. Lee, (1982): A semi-empirical sea-spectrum model for scattering coefficient estimation, IEEE J. Oceanic Eng., Vol. OE-7, No. 4, 166-176.

Gabarro, C., J. Font, A. Camps, M. Vall-Llossera, and A. Julia, (2004): A new empirical model of sea surface microwave emissivity for salinity remote sensing Geophysical Research Letters, vol. 31, no. 1, pp. 5.

Gaiser, P.W., and Coauthors (2004): The WindSat Spaceborne Polarimetric Microwave Radiometer: Sensor Description and early Orbit Performance. *IEEE Trans. Geo. Rem. Sens.*, **42**, 2347-2361, DOI: 10.1109/TGRS.2004.836867.

Guillou, C., English, S. J., Prigent, C., & Jones, D. C., (1996): Passive microwave airborne measurements of the sea surface response at 89 and 157 GHz. *Journal of Geophysical Research: Oceans*, *101*(C2), 3775-3788.

Guillou, C. et al., (1998): Impact of new permittivity measurements on sea surface emissivity modeling in microwaves, Radio Sci., vol. 33, no. 3, pp. 649–667, 1998.

Hollinger, J. P., (1971): Passive microwave measurements of sea surface roughness. *IEEE Transactions on Geoscience Electronics*, *9*(3), 165-169.

Hwang, P., N. Reul, T. Meissner, S. Yueh, (2019): Ocean Surface Foam and Microwave Emission: Dependence on Frequency and Incidence Angle, IEEE Trans. Geosci. Remote Sens., Vol. 57, No. 10, pp. 8223-8234, DOI: 10.1109/TGRS.2019.2919001

Hwang, P. A., Anguelova, M. D., Burrage, D. M., Wang, D. W., Wesson, J. C., Division, R. S., & Division, O., (2012): Effects of foam and wind and wind waves on microwave ocean emission, IGARSS, 2591–2594. 10.1109/IGARSS.2012.6350949.

Irisov, I.G., A. V. Kuzmin, M. N. Pospelov, J. G. Trokhimovsky, and V. S. Etkin, (1992): The dependence of sea brightness temperature on surface wind direction and speed. Theory and Experiment, in *Proc. IEEE Int. Geoscience and Remote Sensing Symp*., Houston.

Kazumori, M., Liu, Q., Treadon, R. and Derber, J.C., (2008): Impact study of AMSR-E radiances in the NCEP global data assimilation system. Monthly weather review, 136(2), pp.541-559.

Kazumori, M. and English, S.J., (2015): Use of the ocean surface wind direction signal in microwave radiance assimilation. Q.J.R. Meteorol. Soc., 141: 1354-1375. doi:10.1002/qj.2445

Kilic, L., Prigent, C., Boutin, J., Meissner, T., English, S., & Yueh, S., (2020): Comparisons of Ocean Radiative Transfer Models with SMAP and AMSR2 Observations. *Journal of Geophysical Research: Oceans*. In Press.

Klein, L. A., & Swift, C. T., (1977): An improved model for the dielectric constant of sea water at microwave frequencies, *AP-25*(1), 104–111.

Kudryavtsev, V. N., V. K. Makin, and B. Chapron, (1999): Coupled sea surface-atmosphere model 2. Spectrum of short wind waves, J. Geophysical Res., Vol. 104, No. C4, 7625-7639.

Kudryavtsev, V. N., D. Hauser, G. Caudal, and B. Chapron, (2003): A semiempirical model of the normalized radar cross-section of the sea surface, 1. Background model, J. Geophys. Res., Vol. 108, No. C3, 8054, doi: 10.1029/2001JC001003.

Kudryavtsev, V. N., D. Hauser, G. Caudal, and B. Chapron, (2003): A semi-empirical model of the normalized radar cross-section of the sea surface, 2. Radar modulation transfer function, J. Geophys. Res., Vol. 108, No. C3, 8055, doi: 10.1029/2001JC001004.

Lang, R. H., Dinnat, E. P., & Le Vine, D. M., (2017): L-Band Model Function of the Dielectric Constant of Seawater. *IEEE Transactions on Geoscience and Remote Sensing*, *55*(12), 6964–6974. https://doi.org/10.1109/TGRS.2017.2737419

Lang, R. et al., (2016): Accurate measurements of the dielectric constant of seawater at L band, Radio Science, vol. 51, no. 1, pp. 2-24.

Liu, Q., F. Weng and S. J. English, (2011): An Improved Fast Microwave Water Emissivity Model, in IEEE TGRS, vol. 49, no. 4, pp. 1238-1250.

Masuda, K., Takashima, T., & Takayama, Y., (1988): Emissivity of pure and sea waters for the model sea surface in the infrared window regions. *Remote Sensing of Environment*, *24*(2), 313-329.

Masuda, K., (2006): Infrared sea surface emissivity including multiple reflection effect for isotropic Gaussian slope distribution model, Remote Sensing of Environment, Volume 103, Issue 4, 488-496, ISSN 0034-4257, https://doi.org/10.1016/j.rse.2006.04.011.

Meissner, T., and F. Wentz, (2004): The complex dielectric constant of pure and sea water from microwave satellite observations, IEEE TGRS, vol. 42(9), pp 1836.

Meissner, T., and F.J. Wentz, (2012): The Emissivity of the Ocean Surface Between 6 and 90 GHz Over a Large Range of Wind Speeds and Earth Incidence Angles, *IEEE Trans. Geo. and Rem. Sens.*, **50**, 3004-3026, DOI: 10.1109/TGRS.2011.2179662.

Meissner, T., F. Wentz, and L. Ricciardulli, (2014): The emission and scattering of L-band microwave radiation from rough ocean surfaces and wind speed measurements from Aquarius, J. Geophys. Res. Oceans, vol. 119, doi:10.1002/2014JC009837.

Meissner, T., Wentz, F. J., Scott, J., Vazquez-Cuervo, J., (2016): Sensitivity of Ocean Surface Salinity Measurements From Spaceborne L-Band Radiometers to Ancillary Sea Surface Temperature, in IEEE Transactions on Geoscience and Remote Sensing, vol. 54, no. 12, pp. 7105-7111, doi: 10.1109/TGRS.2016.2596100.

Meissner, T, F. Wentz, and D. LeVine, (2018): The Salinity Retrieval Algorithms for the NASA Aquarius Version 5 and SMAP Version 3 Releases, Remote Sensing, 10, 1121, doi:10.3390/rs10071121.

Minnett P.J., A. Alvera-Azcárate, T.M. Chin, G.K. Corlett, C.L. Gentemann, I. Karagali, X. Li, A. Marsouin, S. Marullo, E. Maturi, R. Santoleri, S. Saux Picart, M. Steele, J. Vazquez-Cuervo, (2019): Half a century of satellite remote sensing of sea-surface temperature, Remote Sensing of Environment, Volume 233, 111366, ISSN 0034-4257, https://doi.org/10.1016/j.rse.2019.111366.

Monahan, E. C., & O'Muircheartaigh, I. G., (1986): Whitecaps and the passive remote sensing of the ocean surface. *International Journal of Remote Sensing*, *7*(5), 627–642.

Mouche, A. A., Hauser, D., Daloze, J. F., & Guérin, C., (2005): Dual-polarization measurements at C-band over the ocean: Results from airborne radar observations and comparison with ENVISAT ASAR data. *IEEE Transactions on Geoscience and Remote Sensing*, *43*(4), 753-769.

Nalli, N.R., Minnett, P.J. and Van Delst, P., (2008): Emissivity and reflection model for calculating unpolarized isotropic water surface-leaving radiance in the infrared. I: Theoretical development and calculations. Applied optics, 47(21), pp.3701-3721.

Nalli, N.R., Minnett, P.J., Maddy, E., McMillan, W.W. and Goldberg, M.D., (2008). Emissivity and reflection model for calculating unpolarized isotropic water surface-leaving radiance in the infrared. 2: Validation using Fourier transform spectrometers. Applied optics, 47(25), pp.4649-4671.

Newman, S.M.; Smith, J.A.; Glew, M.D.; Rogers, S.M.; Taylor, J.P., (2005): Temperature and salinity dependence of sea surface emissivity in the thermal infrared. Q. J. R. Meteorol. Soc., 131, 2539–2557. doi: 10.1256/qj.04.150.

Nordberg, W., Conaway, J., & Thaddeus, P., (1969): Microwave observations of sea state from aircraft. *Quarterly Journal of the Royal Meteorological Society*, *95*(404), 408-413.

Nunziata, F., Sobieski, P., & Migliaccio, M., (2009): The two-scale BPM scattering model for sea biogenic slicks contrast. *IEEE Transactions on Geoscience and Remote Sensing*, *47*(7), 1949-1956.

Nghiem, S. V., F. K. Li, S.-H., Lou, G. Neumann, R. E. McIntosh, S. C. Carson, J. R. Carswell, E. J. Walsh, M. A. Donelan, and W. M. Drennan, (1995): Observations of Radar Backscatter at Ku and C Bans in the Presence of Large Waves during the Surface Wave Dynamcis Experiment, IEEE Trans. Geosci. Remote Sens., Vol. 33, No. 3, pp. 708-721.

Phalippou, L., (1996): Variational retrieval of humidity profile, wind speed and cloud liquid-water path with the SSM/I: Potential for numerical weather prediction. *Quarterly Journal of the Royal Meteorological Society*, *122*(530), 327-355.

Pierson, W. J and R. A. Stacy, (1973): The elevation, slope, and curvature spectra of a wind roughened sea surface, Contract Rep. NASA CR-2247, Langley Res. Center, NASA, Hampton, Va..

Prigent, C., Abba, P., & Cheudin, M., (1988): A quasi-optical polarization rotator. *International journal of infrared and millimeter waves*, *9*(5), 477-490.

Prigent, C., Aires, F., Wang, D., Fox, S., & Harlow, C., (2017): Sea-surface emissivity parametrization from microwaves to millimetre waves. *Quarterly Journal of the Royal Meteorological Society*, *143*(702), 596-605.

Qiao, Tai, Tsang, Leung, Vandemark, Douglas, Liao, T.H., Nouguier, F., Chapron, B., (2018): Sea Surface Radar Scattering at L-Band Based on Numerical Solution of Maxwell's Equations in 3-D (NMM3D), IEEE Trans. Geoscience and Remote Sensing, Volume: 56 Issue: 6 Pages: 3137-3147.

Quilfen, Y., B. Chapron, F. Collard, D. Vandemark, (2004): Relationship between ERS Scatterometer Measurement and Integrated Wind and Wave Parameters. *J. Atmos. Oceanic Technol.*, 21, 368–373. doi: 10.1175/1520-0426(2004)021.

Saunders, R., Hocking, J., Turner, E., Rayer, P., Rundle, D., Brunel, P., Vidot, J., Roquet, P., Matricardi, M., Geer, A., Bormann, N., and Lupu, C., (2018): An update on the RTTOV fast radiative transfer model (currently at version 12), Geosci. Model Dev., 11, 2717–2737, https://doi.org/10.5194/gmd-11-2717-2018, 2018.

Semyonov, B. I., (1966): Approximate computation of scattering of electromagnetic waves by rough surface contours, *Radio Eng. Electron Phys.*, 11, pp. 1179–1187.

Stogryn, A., (1967): The apparent temperature of the sea at microwave frequencies. *IEEE Transactions on Antennas and Propagation*, *15*(2), 278-286.

Stogryn, A., (1997): *Equations for the permittivity of sea water*.

Stogryn, A. P., Bull, H. T., Rubayi, K., & Iravanchy, S., (1995): *The microwave dielectric properties of sea and fresh water*.

Swadley, S., G, Poe., D. Kunkee, W. Bell, S. Brown, I. Prata, E. Long, and D. Boucher (2008): SSMIS calibration anomalies: Observed F-16 and F-17 anomalies, detailed analysis of the root causes, and the path forward. Proc. 16th Int. TOVS Study Conf., Angra dos Reis, Brazil, Int. TOVS Working Group.

Tang, C. (1974): The effect of droplets in the air-sea transition zone on the sea brightness temperature, *J. Phys. Oceanogr.*, vol. 4, no. 4, pp. 579-593.

Tang, W., Yueh, S., Yang, D., Fore, A., Hayashi, A., Lee, T., Fournier, S., Holt, B., (2018): The Potential and Challenges of Using Soil Moisture Active Passive (SMAP) Sea Surface Salinity to Monitor Arctic Ocean Freshwater Changes, Remote Sensing,10.3390/rs10060869.

Wackermann, C. C., P. Clemente-Colon, W. G. Pichel, X. F. Li, (2002): A two-scale model to predict C-band VV and HH normalized radar cross section values over the ocean, Canadian J. Remote Sens., Vol. 28, pp. 367-384.

Waldteufel, P., Vergely, J. L., & Cot, C., (2004): A modified cardioid model for processing multiangular radiometric observations. *IEEE Transactions on Geoscience and Remote Sensing*, *42*(5), 1059–1063. https://doi.org/10.1109/TGRS.2003.821698

Webster Jr, W. J., Wilheit, T. T., Ross, D. B., & Gloersen, P. (1976): Spectral characteristics of the microwave emission from a wind-driven foam-covered sea. *Journal of Geophysical Research*, *81*(18), 3095-3099.

Weng, F. Z., X. W. Yu, Y. H. Duan, J. Yang, and J. J. Wang, (2020): Advanced Radiative Transfer Modeling System (ARMS): A new-generation satellite observation operator developed for numerical weather prediction and remote sensing applications. Adv. Atmos. Sci., 37(2), https://doi.org/10.1007/s00376-019-9170-2.

Weng, F., and H. Yang, (2016): Validation of ATMS calibration accuracy using Suomi NPP Pitch Maneuver Observations, Remote Sensing, *8*(4), 332; doi:10.3390/rs8040332

Wentz, F. J., (1975): A two-scale scattering model for foam-free sea microwave brightness temperatures. *Journal of Geophysical Research*, *80*(24), 3441-3446.

Wieliczka, D.M., Weng, S. and Querry, M.R., (1989): Wedge shaped cell for highly absorbent liquids: infrared optical constants of water. Applied optics, 28(9), pp.1714-1719.

Wilheit, T. T., (1979): A model for the microwave emissivity of the ocean's surface as a function of wind speed. *IEEE Transactions on Geoscience Electronics*, *17*(4), 244-249.

Wilson, W. J., Li, F. K., Njoku, E. G., Rahmat- Samii, Y., (2001): Error sources and feasibility for microwave remote sensing of ocean surface salinity. IEEE Transactions on Geoscience and Remote Sensing, vol. 39, no. 5, pp. 1049-1060.

Wu, S. T. and A. K. Fung, (1972): A noncoherent model for microwave emissions and backscattering from the sea surface, *J. Geophy. Res.*, vol. 77, no. 30, pp. 5917–5929.

Wu, X., & Smith, W. L., (1997). Emissivity of rough sea surface for 8–13 µm: modeling and verification. *Applied optics*, *36*(12), 2609-2619.

Yin, X., Boutin, J., Dinnat, E., Song, Q., & Martin, A., (2016): Roughness and foam signature on SMOS-MIRAS brightness temperatures: A semi-theoretical approach. *Remote Sensing of Environment*, *180*, 221–233. https://doi.org/10.1016/j.rse.2016.02.005

Yueh, S., (1997): Modeling of wind direction signals in polarimetric sea surface brightness temperatures. IEEE Transactions on Geoscience and Remote Sensing, 35(6), 1400–1418.

Yueh, S. H., W. Tang, A. Fore, G. Neumann, A. Hayashi, A. Freedman, J. Chaubell, and G. Lagerloef, (2013): L-band Passive and Active Microwave Geophysical Model Functions of Ocean Surface Winds and Applications to Aquarius Retrieval. *IEEE Trans. Geoscience and Remtoe Sensing*, 51 (9), 4619-4632, DOI: 10.1109/TGRS.2013.2266915.

Yueh, S. H., W. Tang, A. Fore, A. Hayashi, Y. T. Song, and G. Lagerloef, (2014): Aquarius geophysical model function and combined active passive algorithm for ocean surface salinity and wind retrieval, *J. Geophys. Res. Oceans,* 119, 5360–5379, doi:10.1002/2014JC009939.

Yueh, S. H., W. Tang, A. G. Fore, and A. Hayashi, (2015): Impact of Ocean Wave Height on L-band Passive and Active Microwave Observations of Sea Surfaces, IEEE J. Selected Topics in Applied Earth Obs. Remote Sens., Vol. 8, No. 12, pp. 5491-5499.

Yueh, S., Alexander Fore, Wenqing Tang, Hayashi Akiko, Bryan Stiles, Nicolas Reul, Yonghui Weng and Fuqing Zhang, (2016): SMAP EQUATION CHAPTER 1 SECTION 1L-Band Passive Microwave Observations of Ocean Surface Wind During Severe Storms, IEEE Trans Geosci. Remote Sens., vo.. 54, no. 12, pp. 7339-7350.

Zhou, Y., Lang, R. H., Dinnat, E. P., & Le Vine, D. M., (2017): L-band model function of the dielectric constant of seawater. *IEEE Transactions on Geoscience and Remote Sensing*, *55*(12), 6964-6974.